Bifurcations and Patterns in Compromise Processes

E. Ben-Naim*

Theoretical Division and Center for Nonlinear Studies,
Los Alamos National Laboratory, Los Alamos, New Mexico, 87545

P. L. Krapivsky[†] and S. Redner[‡]

Center for BioDynamics, Center for Polymer Studies,
and Department of Physics, Boston University, Boston, MA, 02215

We study an opinion dynamics model in which agents reach compromise via pairwise interactions. When the opinions of two agents are sufficiently close, they both acquire the average of their initial opinions; otherwise, they do not interact. Generically, the system reaches a steady state with a finite number of isolated, noninteracting opinion clusters ("parties"). As the initial opinion range increases, the number of such parties undergoes a periodic sequence of bifurcations. Both major and minor parties emerge, and these are organized in alternating pattern. This behavior is illuminated by considering discrete opinion states.

I. INTRODUCTION

In a society, people typically have a wide range of opinions. However, individual opinions on a particular issue are not static but rather evolve due to the influences of acquaintances or other external factors. In principle, opinions could evolve *ad infinitum*, consensus could emerge, or a population could reach a state that consists of a finite set of distinct opinion clusters, or "parties".

It is natural to discuss this process within the framework of interacting particle systems [1, 2]. A classic example is the voter model where agents, who possess two possible opinions, adopt the state of a randomly selected neighbor [2–4]. Individual opinions evolve until consensus is eventually reached, and the probability that a given opinion ultimately wins is equal to the initial fraction of agents with that opinion [4]. Several other Ising-type opinion models, incorporating more realistic features, have been proposed recently [5–10].

In this paper, we study the compromise model, a simple model for the evolution of opinions in a heterogeneous population [11, 12]. To account for the diversity of the population, the opinion is either a real-valued variable or a discrete variable with many states [13–15]. To mimic the natural human tendency for reaching a fair compromise, in an interaction between two agents, both acquire the average of their initial opinions. Last, to incorporate self confidence or conviction in one's own opinion, interactions between agents whose opinion difference is larger than some threshold are forbidden.

Monte Carlo simulations of the compromise model have shown that either consensus or diversity can arise, depending on system parameters [11, 12]. Here, we investigate the compromise model using numerical integration of the governing rate equations for continuum opinions and analytical solutions for discrete opinions. Numerical integration is more efficient than direct numerical simulation and provides better resolution of the time dependent and steady state behaviors.

We find that the compromise model exhibits a rich behavior. In the long-time limit, the system condenses into a finite set of equally-spaced opinion clusters (parties), with the population in adjacent clusters alternating between two values that differ by 4 orders of magnitude. As the initial range of opinions grows, the number of parties increases via a periodic sequence of bifurcations. The corresponding period governs the basic features of the emergent structure, namely, the size of the major clusters, and their separation. Near bifurcation points, the size of minor clusters vanishes algebraically, and we provide a heuristic explanation for this behavior.

Underlying the compromise model is a stochastic averaging process. Closely related averaging processes naturally arise in diverse systems, including one-dimensional inelastic collisions [16, 17], dynamics of headways in traffic flows [18, 19], mass transport [20], force fluctuations in bead packs [21], wealth exchange processes [22, 23], and the Hammersley process [24, 25]. While our findings are discussed in the framework of opinion dynamics, they may very well be relevant in these different contexts.

In Sec. II, we describe the numerical integration of the rate equations for the opinion probability density and the resulting bifurcations. In Sec. III, we examine systems with a finite number N of discrete and equally-spaced opinions. When N is relatively small, these systems can be treated analytically, thereby illuminating the behavior in the continuum case. Generally, consensus is reached for small enough N, while a state with several distinct non-interacting clusters is reached for large N. We conclude in Sec. IV.

---

*Electronic address: `ebn@lanl.gov`
[†]Electronic address: `paulk@bu.edu`
[‡]Electronic address: `redner@bu.edu`

II. THE CONTINUUM VERSION

In the continuum version of the compromise model, each agent is initially assigned an opinion x from some specified distribution. Randomly selected pairs of agents undergo sequential interactions. Such interactions are restricted to agents whose opinion difference lies below a threshold that is set to unity without loss of generality. When agents with opinions x_1 and x_2 interact, both acquire the average opinion:

$$(x_1, x_2) \to \left(\frac{x_1 + x_2}{2}, \frac{x_1 + x_2}{2} \right) \qquad |x_2 - x_1| < 1, \quad (1)$$

while if $|x_2 - x_1| > 1$, no interaction occurs. This model is essentially identical to that of Refs. [11, 12].

Let us denote by $P(x,t)\,dx$ the fraction of agents that have opinions in the range $[x, x + dx]$ at time t. The distribution $P(x,t)$ evolves according to the rate equation

$$\frac{\partial}{\partial t} P(x,t) = \int\!\!\int_{|x_1-x_2|<1} dx_1 dx_2 P(x_1,t)P(x_2,t)$$
$$\times \left[\delta\left(x - \frac{x_1+x_2}{2} \right) - \delta(x - x_1) \right]. \quad (2)$$

The quadratic integrand reflects the binary nature of the interaction and the gain and loss terms reflect the process (1). This basic dynamical rule conserves the total mass and the mean opinion. That is, M_0 and M_1, the first two moments of the opinion distribution are conserved, where $M_k(t) \equiv \int dx\, x^k\, P(x,t)$ is the kth moment of the distribution. We restrict our attention to flat initial distributions $P_0(x) \equiv P(x,0) = 1$ for $x \in [-\Delta, \Delta]$. Our goal is to determine the nature of the final state $P_\infty(x) \equiv P(x,\infty)$.

When all agents interact, namely, when $\Delta < 1/2$, the rate equations are integrable [16, 17]. In particular, the second moment obeys $\dot{M}_2 + M_0 M_2/2 = M_1^2$, where the overdot denotes time derivative. Using $M_1 = 0$, we find that the second moment vanishes exponentially in time:

$$M_2(t) = M_2(0)\, e^{-M_0 t/2}, \quad (3)$$

with $M_0 = 2\Delta$. Thus all agents approach the center opinion and the system eventually reaches the consensus

$$P_\infty(x) = M_0 \delta(x). \quad (4)$$

The distribution $P(x,t)$ approaches the localized state (4) in a self-similar fashion, $P(x,t) \simeq \frac{2M_0}{\pi w}\left(1 + z^2\right)^{-2}$ with variance $w = M_2^{1/2}/M_0$ and scaling variable $z = x/w$ [17].

For larger values of Δ, the opinion distribution does not condense into a single cluster, but rather the distribution evolves into "patches" that are separated by a distance larger than one. This behavior results from an instability that propagates from the boundary toward the
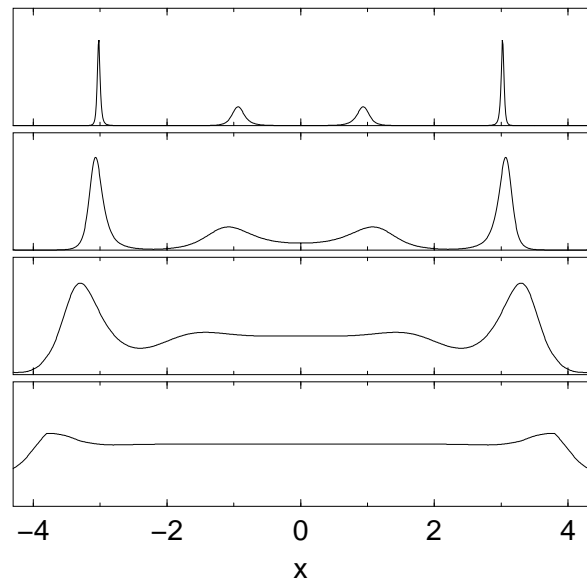

FIG. 1: Evolution of the opinion distribution for $\Delta = 4.3$ where four major clusters ultimately arise (see Fig. 2). Shown is $P(x,t)$ versus x for times $t = 0.5$ (bottom), 3, 6, and 9 (top).

center (Fig. 1). Once each patch is isolated, it then separately evolves into a delta function as in the $\Delta < 1/2$ case. The final distribution consists of a series of non-interacting clusters at locations x_i with masses m_i:

$$P_\infty(x) = \sum_{i=1}^{p} m_i\, \delta(x - x_i) \quad (5)$$

with $\sum m_i = M_0 = 2\Delta$ and $\sum m_i x_i = M_1 = 0$ to satisfy the conservation laws.

Our goal is to understand basic characteristics of the final state. How many clusters arise? Where are they located (in opinion space)? What are their masses? As we shall see, the answers to these questions depend in a surprisingly complex manner on the single control parameter, the initial opinion range Δ.

A. Cluster Locations

To determine how the final state depends on Δ, we numerically integrated the rate equation (2) by discretizing x into 400Δ equally-spaced states. The range $0 < \Delta < 10$ was investigated using a fine mesh (0.0025 increments). The rate equations were integrated using a fourth order Adams-Bashforth method [26] up to a sufficiently long time that the probability distribution separated into noninteracting patches. Then, the two conservation laws were invoked to determine the ultimate mass and location of each patch. The accuracy was 10^{-9} in $P(x,t)$.

The cluster locations exhibit a striking regularity, as seen in plotting x_i versus Δ (Fig. 2). There are three types of clusters: major clusters (mass $M > 1$), minor
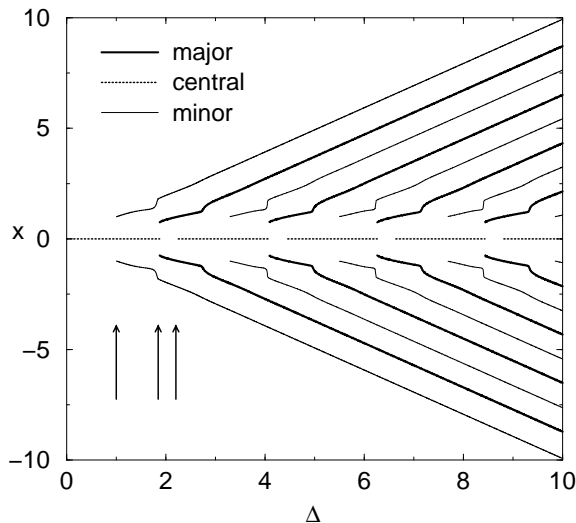
FIG. 2: Location of final state clusters versus the initial opinion range Δ. The three types of clusters, defined in the text, are noted. The vertical arrows indicate the location of the first 3 bifurcations.

clusters (mass $m < 10^{-2}$), and a central cluster located exactly at $x = 0$. The number of clusters grows via a series of bifurcations. When $\Delta < 1/2$, the final state is a single peak located at the origin, and this situation persists as long as $\Delta < 1$. When Δ exceeds one, two new clusters are born at the extreme edges, $x \approx \pm\Delta$. As Δ increases, further bifurcations of three basic types occur:

1. Nucleation of a symmetric pair of clusters: $\emptyset \rightarrow \{-x, x\}$ with $x = 1$.

2. Annihilation of a central cluster and simultaneous nucleation of a symmetric pair of clusters: $\{0\} \rightarrow \{-x, x\}$ with $x \approx 0.75$.

3. Nucleation of a central cluster: $\emptyset \rightarrow \{0\}$.

The bifurcations always occur in a periodic order: $1, 2, 3, 1, 2, 3, \ldots$. Numerically, the first 4 generations of bifurcations are located at

$$(\Delta_1, \Delta_2, \Delta_3) = \begin{cases} (1.000, 1.871, 2.248), \\ (3.289, 4.079, 4.455), \\ (5.496, 6.259, 6.638), \\ (7.676, 8.431, 8.810). \end{cases}$$

Successive bifurcation points of the same type are all separated by the same distance: $\Delta_i(n+1) - \Delta_i(n) \rightarrow$ const. Also, the distance between different types of bifurcations within the same generation eventually becomes constant. Thus the bifurcation diagram, with all its intricate features, repeats in a periodic manner

$$x(\Delta) = x(\Delta + L), \tag{6}$$

with period $L \approx 2.155$. The period was estimated by extrapolating the differences in the locations of the first few
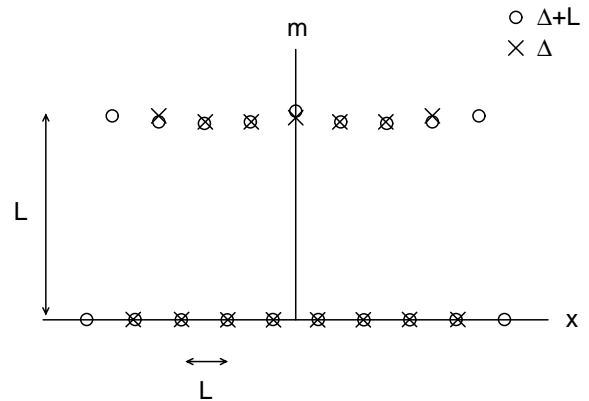

FIG. 3: The masses of the final clusters versus their location for the cases of $\Delta \approx 7.8$ and $\Delta + L \approx 10$. The clusters in the two systems coincide, except that the larger system has four more clusters. The scale of the inter-cluster separations and the masses of the major clusters are indicated.

transitions to ∞. The period characterizes universality in the bifurcation diagram, resembling the Feigenbaum number in the logistic map [27].

In type-1 (2) bifurcations, branches of minor (major) clusters nucleate near the origin, and these persist for all larger Δ. As each branch evolves, notice that it exhibits a large curvature change or a kink due to the effect of a subsequent bifurcation. For $|x| \gtrsim 2$, the branch growth is practically linear with a slope commensurate with the opinion range: $|dx/d\Delta| \rightarrow 1$.

The periodic behavior further implies that the separation between clusters becomes constant. Moreover, when a system of size Δ is compared with a system of size $\Delta + L$, cluster locations in the smaller system coincide with the larger one, as shown in Fig. 3. The larger system, however, contains two additional pairs of major and minor clusters. Thus, the period L governs the overall number of clusters and the separation between them. For $\Delta \gg 1$ there are $4\Delta/L$ clusters, with neighboring clusters separated (approximately) by distance $L/2$.

B. Cluster Masses

An even richer picture emerges when the cluster masses are considered. First, the cluster masses vary periodically in the initial opinion range, that is, $m(\Delta) = m(\Delta + L)$, as seen in Fig. 4. Second, clusters are organized in an alternating major-minor pattern (see Figs. 2 and 3). For large Δ, each cluster mass approaches a constant value. The major clusters, which contain nearly the entire mass in the system, saturate at a value equal to the period, $M \rightarrow L$. The masses of the minor clusters approach a much smaller level: $m \rightarrow 3 \cdot 10^{-4}$ (see Fig. 4). This minute mass implies that a sufficiently large population is needed for minor clusters to exist.

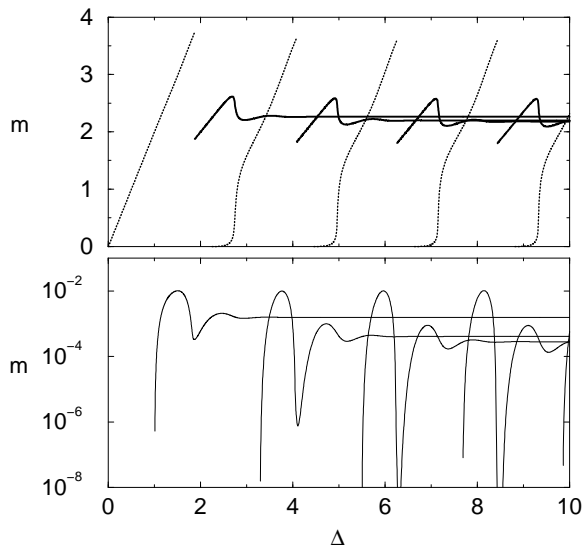The central cluster is special. Its mass never becomes

FIG. 4: Cluster mass versus opinion range. The central clusters (periodic variation) and the major cluster are shown on a linear scale (top), while minor and central clusters are shown on a logarithmic scale (bottom).
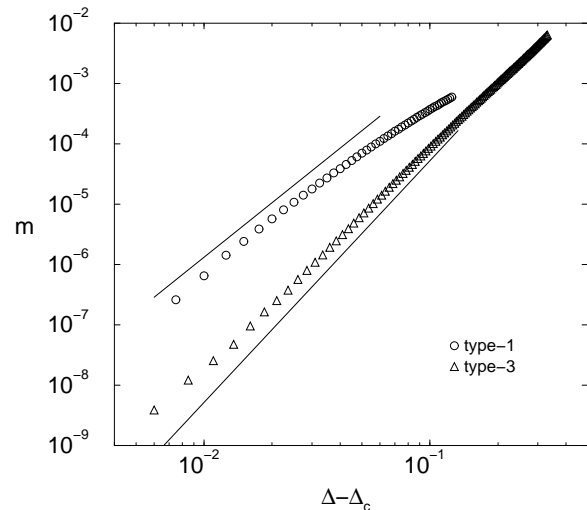

FIG. 5: Critical behavior for the masses of the minor clusters at type-1 (top) and type-3 (bottom) bifurcations. The straight lines have slopes 3 and 4.

constant but instead varies in a periodic manner with Δ (Fig. 4). A central cluster nucleates with an infinitesimal mass at a type-3 bifurcation, grows slowly for a while, then it undergoes an explosive growth until its mass becomes of order unity. Finally, its mass grows linearly with Δ. At some threshold, the central cluster splits into two major clusters via a type-2 bifurcation (Fig. 4). This birth-and-death pattern repeats *ad infinitum*.

The minor clusters exhibit two subtle features. First, the mass of the most extreme cluster saturates to a mass m' that is approximately one order of magnitude greater than all other minor clusters. Second, the mass of the minor clusters varies non-monotonically with Δ and there is a small range of Δ, where the mass of a newly-born minor cluster suddenly drops (Fig. 4) before the mass saturates to a constant value. We are unable to resolve whether there is a finite gap or just a singular point where the mass vanishes.

At type-1 and type-3 bifurcations, new clusters form, and the mass of these nascent clusters vanishes algebraically according to

$$m \sim (\Delta - \Delta_n)^{\alpha_n} \qquad (7)$$

as $\Delta \to \Delta_n$. The exponent depends only on the type n of the bifurcation point; numerically we find $\alpha_1 \approx 3$ and $\alpha_3 \approx 4$ (Fig. 5). We now give a heuristic explanation for this behavior.

To understand the behavior near a type-1 bifurcation, consider the very first one at $\Delta_1 = 1$. Let $\Delta = 1 + \epsilon$ with $\epsilon \to 0$. It is convenient to divide the total opinion range $(-\Delta, \Delta)$ into a central subinterval $(-1, 1)$ and two boundary subintervals: $(1, 1 + \epsilon)$ and $(-1 - \epsilon, -1)$. Let $m(t)$ be the mass in a boundary subinterval. Initially,

$m(0) = \epsilon$. Such mass is lost due to interaction with one half of the central subinterval. As a result, $\dot{m} = -m$, which gives

$$m(t) = \epsilon\, e^{-t}. \qquad (8)$$

On the other hand, the mass of the central subinterval gets concentrated in a region near the origin whose spread $w(t)$ decreases with time. At some moment t_f the separation between masses in the central and boundary subintervals exceeds unity. We anticipate that the mass in the boundary subinterval converges to its center $x = 1 + \epsilon/2$, and hence, this critical separation occurs when $w(t_f) \sim \epsilon/2$. For $t \gg t_f$, the interaction between the two subintervals stops and the mass of the emerging minor cluster freezes at $m_f \sim \epsilon\, e^{-t_f}$.

The spread $w(t)$ can be estimated by noting that to zeroth order in ϵ, (i) the central subinterval is not affected by the boundary subintervals, and (ii) eventually, almost all agents are within the interaction range. Therefore, the asymptotic behavior is the same as in the case $\Delta < 1/2$, and the spread follows directly from the second moment (3), $w(t) \sim M_2^{1/2} \sim e^{-t/2}$ since $\Delta = 1 + \epsilon \cong 1$. Using the stopping criteria, $w(t_f) \sim e^{-t_f/2} \sim \epsilon$, the final minor cluster mass is $m_f \sim \epsilon\, e^{-t_f} \sim \epsilon^3$, leading to $\alpha_1 = 3$.

Consider now a type-3 bifurcation that occurs at some Δ_3. We write $\Delta = \Delta_3 + \epsilon$ and adapt our previous argument. Let $m(t)$ be the mass of the newly-formed central cluster, and let M be the final mass of the two major clusters surrounding it. We have $\dot{m} = -mM$, since the central cluster interacts with half of the mass M on either sides. Therefore

$$m(t) \sim e^{-Mt}. \qquad (9)$$

In contrast to Eq. (8) where the amplitude was of order ϵ, the amplitude in Eq. (9) is of order unity. This

arises because the range of opinions that contributes to the ultimate central cluster is of the order of the interaction range. Now the argument proceeds as before. The width of the large cluster varies as $e^{-Mt/4}$. The condition for the central cluster and its neighbors to decouple is $e^{-Mt_f/4} \sim \epsilon$. At this point, we have $m_f \sim e^{-Mt_f} \sim \epsilon^4$, resulting in the exponent $\alpha_3 = 4$.

The heuristic argument we have presented is consistent with the extremely small mass of the minor clusters. For large Δ, the system is governed by the parameter $\tilde{\epsilon} \equiv \frac{1}{2}L - 1 \approx 0.08$, the excess between the adjacent cluster separation and the interaction range. This parameter essentially plays the role of ϵ, the small distance from a bifurcation point. The two extreme minor clusters evolve according to the mechanism that led to the ϵ^3 behavior near a type-1 bifurcation. Thus, their mass can be estimated $m' \sim \tilde{\epsilon}^3 \approx 5 \cdot 10^{-4}$. On the other hand, minor clusters in the bulk evolve according to the mechanism that led to the ϵ^4 behavior near a type-3 bifurcation. Accordingly, their mass is estimated by $m \sim \tilde{\epsilon}^4 \approx 4 \cdot 10^{-5}$, again a reasonable value.

III. THE DISCRETE VERSION

Often, one faces a choice among a finite set of options, so it is natural to consider a discrete version of the compromise model. While interesting on its own, the discrete model also enables us to illuminate many qualitative aspects of the behavior in the continuum case. Discrete systems are governed by a finite set of non-linear rate equations, so explicit solutions are generally impossible. Nevertheless, we can gain considerable insight by investigating small systems, using stability analysis and related tools from theory of ordinary differential equations [28].

In the discrete version, each agent can take on an opinion from a set of N equally-spaced values. To impose an interaction threshold and also to ensure that the outcome of an interaction remains within the state space, two agents interact as follows: (a) If the opinion difference is greater than two, there is no interaction. (b) If the difference equals two, the agents reach a fair compromise and each takes on the average opinion value. (c) If the opinion difference equals one, nothing happens.

We label the opinion states as $i = 1, 2, \ldots, N$, so schematically, in a compromise event $(i-1, i+1) \rightarrow (i, i)$. Denote by $P_i(t)$ the fraction of the population that has opinion state i at time t. For general N the fractions $P_i(t)$ obey the rate equations

$$\dot{P}_i = 2P_{i-1}P_{i+1} - P_i(P_{i-2} + P_{i+2}). \quad (10)$$

This equation formally applies for i at least 2 spacings away from the boundaries (at 1 and N). Setting $P_{-1} = P_0 = P_{N+1} = P_{N+2} \equiv 0$ in Eq. (10), yields the governing equations near the boundaries: $\dot{P}_1 = -P_1P_3$, $\dot{P}_2 = 2P_1P_3 - P_2P_4$, $\dot{P}_N = -P_NP_{N-2}$, and $\dot{P}_{N-1} = 2P_NP_{N-2} - P_{N-1}P_{N-3}$. Again, the fractions $P_i(t)$ sat-

isfy two conservation laws:

$$\sum_{i=1}^{N} P_i = 1, \qquad \sum_{i=1}^{N} iP_i = A, \quad (11)$$

with $1 \le A \le N$. The former (latter) reflects conservation of the total population (opinion). As a result, there are $N - 2$ independent variables for an N-state system.

A. Typical Behavior

Equations (10) are non-linear and therefore for $N \ge 4$ they cannot be solved to obtain explicit formulae for $P_i(t)$. However, the qualitative behavior can be still understood. For example, Eqs. (10) admit only the simplest type of attractors – fixed points – while limit cycles are impossible. We illustrate this by analyzing small values of N to highlight the new qualitative features that arise as N increases.

1. Isolated fixed points

For $N = 3$, there is a single fixed point located at

$$\begin{cases} (2 - A, A - 1, 0) & \text{when } 1 \le A \le 2, \\ (0, 3 - A, A - 2) & \text{when } 2 \le A \le 3. \end{cases}$$

This point is *stable*. Asymptotically, it is approached exponentially fast in time; *e.g.*, for $1 < A < 2$ one finds $P_3 \propto e^{-(2-A)t}$. An exception arises for the symmetric initial condition ($A = 2$) when the final central state $(0, 1, 0)$ is approached algebraically in time: $P_1 = P_3 \rightarrow t^{-1}$.

For $N = 4$, there is also a single stable fixed point located at

$$\begin{cases} (2 - A, A - 1, 0, 0) & \text{when } 1 \le A \le 2, \\ (0, 3 - A, A - 2, 0) & \text{when } 2 \le A \le 3, \\ (0, 0, 4 - A, A - 3) & \text{when } 3 \le A \le 4. \end{cases}$$

Additionally, there is a fixed point $(\frac{4-A}{3}, 0, 0, \frac{A-1}{3})$ that is always unstable. The stable fixed point is approached exponentially in time.

2. Lines of fixed points

For $N = 5$, some fixed points are no longer isolated but instead they form *lines*. Indeed, Eqs. (10) admit fixed points of the generic forms $(P_1^*, P_2^*, 0, 0, P_5^*)$ and $(P_1^*, 0, 0, P_4^*, P_5^*)$ that are stable when, respectively, $P_1^* > 3P_5^*$ or $P_5^* > 3P_1^*$. Recalling the conservation laws (11) we can write these fixed points in the form

$$\begin{cases} (2 - A + 3P_5^*, A - 1 - 4P_5^*, 0, 0, P_5^*), \\ (P_1^*, 0, 0, 5 - A - 4P_1^*, A - 4 + 3P_1^*) \end{cases} \quad (12)$$

6

and obviously the fixed points form lines. The fixed points (12) from the first line are stable when $1 + 4P_5^* < A < 2$, the fixed points (12) from the second line are stable when $4 < A < 5 - 4P_1^*$. There is also a stable isolated fixed point located at

$$
\begin{cases}
(0, 3-A, A-2, 0, 0) & \text{when } 2 < A \leq 3, \\
(0, 0, 4-A, A-3, 0) & \text{when } 3 \leq A < 4.
\end{cases} \quad (13)
$$

For $2 < A < 4$, every initial condition is in the basin of attraction of the isolated fixed point (13). Therefore we know the fate of the system without explicitly solving the rate equations. This statement tacitly assumes that a trajectory does not approach a limit cycle or other complicated attractor; this will be justified later. In the complementary range $A \in (1,2) \cup (3,4)$ the trajectories approach one of the stable fixed points in (12). For example, if $1 < A < 2$, the final state is $(2 - A + 3P_5^*, A - 1 - 4P_5^*, 0, 0, P_5^*)$ for some $P_5^* \in \left(0, \frac{A-1}{4}\right)$. To determine which fixed point is actually reached depends not only on the initial average opinion $A = \sum i P_i(0)$ but also on other details of the initial condition and requires a complete solution. Qualitatively, for an initial state that is central in character $(2 < A < 4)$, the final occupation fractions are concentrated in a single central cluster consisting of two adjacent sites. Conversely, for an initial state that is biased toward one extreme, the final state consists of two extremal clusters.

The above elementary examples demonstrate a simple principle. The rate equations have multiple stable fixed points. Each stable fixed point is a basin of attraction for some region in the space of initial conditions. The dynamics determine which stable fixed point is eventually approached. In the continuous version, a similar situation occurs where there are enormously many steady states of the form (5). Moreover, we see how depending on the initial conditions, the system can reach a single central cluster or two off-center clusters.

In the remainder of this subsection we consider symmetric situations, $P_i = P_{N+1-i}$. For an N-state system, we can choose $1, 2, \ldots, \lceil N/2 \rceil$ independent states, where $\lceil N/2 \rceil$ is the smallest integer that is larger than or equal to $N/2$. Conservation of population diminishes the number of independent variables by one, while the second conservation law is redundant as $A = (N+1)/2$ always.

3. Explicitly solvable case

For $N = 6$, the rate equations (10) are exactly solvable and the solution neatly illustrates the features described in the previous subsection. Using symmetry and normalization, we can treat the system in the two-dimensional triangular domain defined by (Fig. 6)

$$ \mathcal{T} = \{(P_1, P_2) | P_1 \geq 0, P_2 \geq 0, P_1 + P_2 \leq 1\}. \quad (14) $$

There are two kinds of fixed points: An isolated fixed point $(0,0)$ and a line of fixed points (P_1^*, P_2^*) with $P_1^* +$
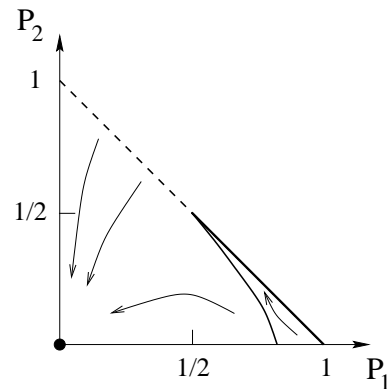

FIG. 6: Schematic (P_1, P_2) phase plane for the symmetric 6-opinion system. Shown are the isolated fixed point (dot), the line of fixed points (heavy line – dashed for unstable and solid for stable), and the separatrix (dotted) that demarcates the basins of attractions of these two sets.

$P_2^* = 1$. Linearizing near the isolated fixed point we find that $\mathbf{P} = (P_1, P_2)^T$ satisfies

$$ \frac{d\mathbf{P}}{dt} = \mathcal{M}\mathbf{P}, \qquad \text{with} \quad \mathcal{M} = \begin{pmatrix} -1 & 0 \\ 2 & -1 \end{pmatrix}, \quad (15) $$

from which the origin is a degenerate stable node. Linearizing near a fixed point (P_1^*, P_2^*) we find that it is stable iff $P_1^* > P_2^*$ and unstable iff $P_1^* < P_2^*$. Thus the isolated fixed point has a finite-area basin of attraction, while every point (P_1^*, P_2^*) with $P_1^* > P_2^*$ has a basin of attraction that is a one-dimensional manifold (Fig. 6). In principle, a two-dimensional system could have closed orbits. However, every closed orbit in a two-dimensional system must enclose fixed points [28]. Here, all fixed points lie on the boundary of the phase plane $\mathcal{T}$, so closed orbits that encircle a fixed point are impossible, thereby ruling out cycles.

The solution to Eqs. (10) for $N = 6$ with symmetric initial conditions is given in the Appendix. This solution gives the following behavior in the phase space $\mathcal{T}$ (see Fig. 5). There is a separatrix (A6) that joins $(P_1, P_2) = (1/2, 1/2)$ with $\left(\sqrt{e/4}, 0\right)$. The part of the phase plane to the left of the separatrix is the basin of attraction of the isolated fixed point, while the complementary region is the basin of attraction of the line of fixed points (P_1^*, P_2^*) with $P_1^* > \frac{1}{2} > P_2^*$. These fixed points are approached exponentially in time. Finally, the separatrix itself is the basin of attraction of the fixed point $(1/2, 1/2)$. In this borderline case the relaxation is algebraic rather than exponential:

$$ P_1 - \frac{1}{2} \to t^{-1}, \quad P_2 - \frac{1}{2} \to -t^{-1}, \quad P_3 \to 2\,t^{-2}. \quad (16) $$

Both consensus and polarization are possible outcomes – which actually occurs depends on the initial condition.

4. Large N

For $N \geq 7$, the systems are $\lceil N/2 \rceil - 1 \geq 3$ dimensional, and already the trajectories of 3-dimensional systems may exhibit a vast range of behaviors including chaos [28, 29]. In the present case, however, we find that there are simply more and more fixed points, and they appear as isolated fixed points, lines, surfaces, and higher-dimensional sub-manifolds.

For $N = 7$, the system is three-dimensional, and the phase space is the simplex

$$\mathcal{S} = \{(P_1, P_2, P_3) | P_j \geq 0, P_1 + P_2 + P_3 \leq 1\}. \quad (17)$$

For simplicity, we denote states by (P_1, P_2, P_3, P_4). The system admits the following fixed points:

1. A line of fixed points $(P_1^*, P_2^*, 0, 0)$ corresponding to a polarized society.

2. A line of fixed points $(P_1^*, 0, 0, P_4^*)$ corresponding to a society with both centrists and extremists.

The second case includes the central consensus state $(0, 0, 0, 1)$ as a special case.

Linearizing around the fixed point $(P_1^*, P_2^*, 0, 0)$ we find that $\mathbf{P} = (P_3, P_4)^T$ satisfies

$$\frac{d\mathbf{P}}{dt} = \mathcal{M}\mathbf{P}, \qquad \mathcal{M} = \begin{pmatrix} -P_1^* & 2P_2^* \\ 0 & -2P_2^* \end{pmatrix}, \quad (18)$$

implying that $(P_1^*, P_2^*, 0, 0)$ is a stable node (we tacitly assume that $P_1^*, P_2^* > 0$; when $P_1^* = 2P_2^*$ this node is degenerate). Linearizing around the fixed point $(P_1^*, 0, 0, P_4^*)$ we find that $\mathbf{P} = (P_2, P_3)^T$ satisfies

$$\frac{d\mathbf{P}}{dt} = \mathcal{M}\mathbf{P}, \qquad \mathcal{M} = \begin{pmatrix} -P_4^* & 2P_1^* \\ 2P_4^* & -P_1^* \end{pmatrix}, \quad (19)$$

implying that $(P_1^*, 0, 0, P_4^*)$ is a saddle point. Therefore the fixed points $(P_1^*, 0, 0, P_4^*)$ are unstable (again it is assumed that $P_1^*, P_4^* > 0$). The two extreme fixed points $(1/2, 0, 0, 0)$ and $(0, 0, 0, 1)$ are *neutrally* stable in the linear approximation. Therefore one must go beyond the linear approximation to probe the stability of consensus. Numerically, one typically finds that the system reaches consensus (*e.g.*, starting from the uniform initial condition). Therefore, consensus appears to be stable.

For larger N, we determined the final state numerically. To compare with the continuum case, we start with the uniform initial condition. Generally, the final state consists of non-interacting clusters. Each cluster consists of a pair of occupied sites and clusters are separated by at least two empty sites. We assign each cluster a mass m equal to the combined occupation of the two sites, and a position x determined from a weighted average.

As a function of N, the number of clusters grows via a series of transitions, rather than bifurcations (Fig. 7). The main difference with the continuum case is that while minor clusters occasionally appear, they do not persist
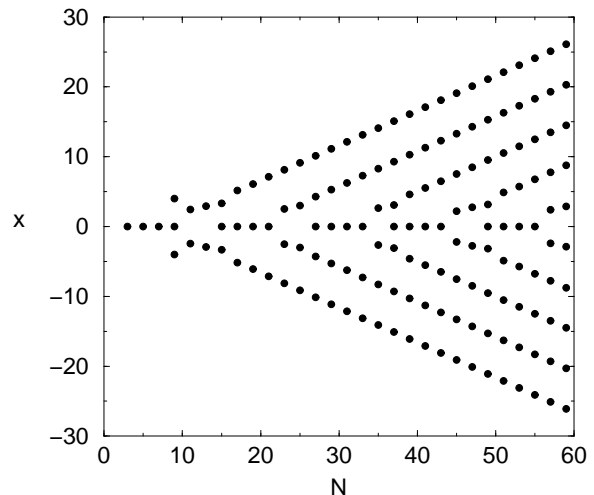

FIG. 7: The location of the final clusters in the discrete model as a function of N, with N odd.

in the form of minor branches. Otherwise, there are many similarities. Transitions involving major and central clusters are observed; in particular, there are type-2 ($\{0\} \rightarrow \{-x, x\}$) and type-3 ($\emptyset \rightarrow \{0\}$) transitions. These transitions are arranged in a periodic structure $2, 3, 2, 3$, and the transition diagram is approximately invariant under the transformation $N \rightarrow N + N_0$ with $N_0 \cong 12$. Branches of major clusters carry almost equal masses, and remarkably, despite the discreteness, these branches grow linearly with N.

B. General Features

1. Volume Contraction

The system of rate equations is dissipative, that is, volumes in phase space contract under the flow. Generally for a system of differential equations $\dot{P}_j = F_j$, a volume $V(t)$ changes according to

$$\frac{dV}{dt} = \int_S \mathbf{F} \cdot \mathbf{n} \, dS = \int_V \nabla \cdot \mathbf{F} \, dV \quad (20)$$

where $\mathbf{n}$ is the outward normal on the bounding surface $S(t)$ that encloses $V(t)$ and $\nabla \cdot \mathbf{F} = \sum_j \frac{\partial F_j}{\partial P_j}$. For the infinite discrete system $\frac{\partial F_j}{\partial P_j} = -P_{j-2} - P_{j+2}$ and thus the contraction rate is twice the (conserved) total population: $-\sum_j \frac{\partial F_j}{\partial P_j} = 2\sum_k P_k$. Hence volumes in phase space shrink exponentially in time. If we set the total population equal to 1, we get $V(t) = V(0) e^{-2t}$.

For finite systems, the contraction rate is generally not a constant but nevertheless volume still shrinks exponentially in time according to the bounds

$$V(0) e^{-2t} \leq V(t) \leq V(0) e^{-t}. \quad (21)$$

For example, for $N = 4$ the contraction rate is $\sum_k P_k = 1$; therefore, $V(t) = V(0)\, e^{-t}$. For $N = 5$, the contraction rate is $1 + P_3$; for $N = 6$, the contraction rate is $1 + P_3 + P_4$, *etc.* This is consistent with the system evolving toward fixed points. Nevertheless, cycles and strange attractors are possible in volume contracting systems, with the celebrated Lorenz system being a prime example [29].

2. Lyapunov functions

We now demonstrate that our system has only fixed points (many of which are actually fixed submanifolds in phase space) by constructing a *Lyapunov function* $L \equiv L[\mathbf{P}(t)]$, *viz.* a smooth function that decreases along trajectories. The existence of a Lyapunov function rules out cycles. Indeed, suppose that there is a periodic solution with period T, then the integral $\int_0^T dt\, \frac{dL}{dt}$ over the period would be negative because the Lyapunov function is decreasing. On the other hand, the integral must be equal to zero since the trajectory returns to the starting point. This contradiction means that no periodic solutions can exist.

Consider, *e.g.*, symmetric situations. For $N = 7$,

$$L = P_4 + 2P_3 + 4P_2 + 8P_1 \qquad (22)$$

is a Lyapunov function; indeed, it satisfies

$$\frac{dL}{dt} = -2P_1 P_3 - 2P_2 P_4, \qquad (23)$$

so the derivative is strictly negative inside the simplex $\mathcal{S}$ (it vanishes only on the two lines of fixed points on the boundary of $\mathcal{S}$).

Generally, we can construct Lyapunov functions for all N. For instance, when N is odd we write $N = 2M - 1$ and verify that

$$L = \sum_{j=1}^{M} 2^{M-j} P_j, \qquad (24)$$

is a Lyapunov function as it satisfies

$$\frac{dL}{dt} = -2P_{M-2}P_M - \sum_{j=1}^{M-3} 2^{M-2-j} P_j P_{j+2}. \qquad (25)$$

3. Negative Diffusion Instability

In the absence of boundaries, any uniform state is a trivial solution of the nonlinear set of the ordinary differential equations (10). To check the stability of the uniform state, $P_i = \text{const.}$, we treat $i \equiv x$ as a continuum variable. Writing $P(x, t) = 1 + \phi(x, t)$ with $\phi(x, t) \ll 1$, this perturbation evolves according to

$$\phi_t + \left(\phi + \frac{7}{6}\phi_{xx} + \frac{1}{2}\phi^2 \right)_{xx} = 0, \qquad (26)$$

where the subscripts denote partial differentiations (a Cahn-Hilliard equation with the energy function $\Psi(\phi) = -\frac{1}{2}\phi^2 - \frac{1}{6}\phi^3$ [30]). To lowest order, this is the diffusion equation with a negative diffusion coefficient. Hence, the uniform state is unstable to the perturbation $\phi(x, t) = \exp(ikx + \lambda t)$ when $k < \sqrt{6/7}$. Therefore, minute details of the initial conditions are magnified, ultimately resulting in isolated clusters. However, the nonlinear terms in Eq. (26) eventually counter the instability. The continuum evolution equation captures the nonlinear evolution of the original discrete system qualitatively but not quantitatively.

IV. DISCUSSION

The interplay between compromise and conviction leads to intriguing opinion dynamics. The system ultimately reaches a static state that consists of a finite number of noninteracting opinion clusters, and the number of these clusters increases via an infinite sequence of self-similar bifurcations as the opinion range increases. In the bulk of the system, clusters are organized in a periodic lattice of alternating minor and major clusters. A central cluster may or may not exist, and its size exhibits a complex periodic behavior.

As a model of mathematical sociology, the compromise model is appealing in its simplicity, yet its behavior is familiar in everyday experience. A political system may or may not contain a centrist party. Alternatively, it may consist of two (or more) off-center parties. Furthermore, the existence of marginal parties halfway between two major ones is also reasonable. Artificial features of the model, such as the identical separation between parties, can be easily circumvented by introducing heterogeneities. For example, since different agents may have different levels of conviction, it may be natural to have interaction thresholds that are specific to each individual.

As a dynamical system, the compromise model exhibits the simplest types of attractors, namely, fixed points that are either sinks or saddles. In the discrete case, we constructed Lyapunov functions and also established that limit cycles and strange attractors are impossible. This conclusion extends to the continuum case. The second moment decreases monotonically with time and hence, it is a Lyapunov functional. Generally, each stable fixed point is the basin of attraction of some region in the space of initial conditions. In other words, the rate equations map an initial state into a final state. Given the large number of these states, it is not obvious how to characterize such a map. One practical approach is to obtain statistical properties of the final state by averaging over all possible initial conditions. In the discrete case, we find that starting from a random initial state ($\{P_i(0)\}$ randomly chosen in the N-dimensional hypercube) the distribution of cluster masses and the distribution of the separations between clusters in the final state are independent of the system size, for large enough systems.

There are important questions concerning robustness of the bifurcation diagram with respect to variations in the dynamical rules or in the initial conditions. The appearance of equally spaced clusters is crucially dependent on the sharp cutoff in the interaction range. Introducing a small concentration of agents who may interact with everybody eventually results in consensus, although multiple clusters can occur on intermediate time scales. The behavior is less sensitive to the details of the averaging procedure. When the opinion difference between two agents is merely reduced by a fixed factor, *i.e.*, they reach partial compromise, an almost identical bifurcation diagram is found.

The initial distribution plays an important role in determining the nature of the final state. We examined in detail exponential initial distributions, $P_0(x) = \exp(-|x|/x_0)$ for $|x| < \Delta$, with the decay constant x_0 of order unity. Major features including the minor-major pattern and the periodic structure of the bifurcation diagram are found for such sharp exponential distributions. However, there are important differences with the flat case. The central cluster always exists and it is major because of the large mass concentrated initially around the origin. New branches of minor and major clusters are nucleated at the boundaries $x = \pm\Delta$ rather than at the vicinity of the origin. Moreover, each minor branch contains a clear gap. This example suggests that there is a number of classes of bifurcation diagrams. A challenging problem is to find classification criteria for the initial conditions.

There are numerous possible generalizations of the compromise model. One is to increase the dimension of the opinion space. Do the final opinions form a lattice? and if yes of what type? Yet another open question is the role of spatial dimension. In the present work, we implemented the mean-field limit where any agents equally well interact with any other agent. However, if agents are located at lattice sites with interactions only between nearest neighbors, spatial correlations are expected to emerge [31, 32]. We anticipate that for the discrete system in which $N \geq N_c(d)$, with $N_c(d)$ depending on the spatial dimension d, the system will freeze into a large number of non-interacting opinion domains. The case of continuum opinions is unexplored, but we expect both slow dynamics and coarsening of opinion patterns as the final state is approached.

Acknowledgments

APPENDIX A: SOLUTION TO THE RATE EQUATIONS FOR $N = 6$

The symmetric $N = 6$ system simplifies after replacement of the time variable t by

$$\tau = \int_0^t dt'\, P_3(t'), \qquad (A1)$$

as the rate equations reduce to the linear system

$$P_1' = -P_1, \quad P_2' = 2P_1 - P_2, \quad P_3' = P_2 - P_1,$$

where $' \equiv d/d\tau$. Solving these equations we obtain

$$
\begin{aligned}
P_1(\tau) &= P_1(0)\, e^{-\tau}, \\
P_2(\tau) &= [2P_1(0)\,\tau + P_2(0)]\, e^{-\tau}, \qquad (A2) \\
P_3(\tau) &= 1 - [2P_1(0)\,\tau + P_1(0) + P_2(0)]\, e^{-\tau}.
\end{aligned}
$$

Depending on the initial conditions, $P_3(\tau)$ either remains positive or it reaches zero. In the former case, $P_3(\tau) \to 1$ as $\tau \to \infty$ and asymptotically the isolated fixed point is reached. To determine the approach to the fixed point in terms of original time variable we write

$$t = \int_0^\tau \frac{d\tau'}{P_3(\tau')}, \qquad (A3)$$

with P_3 given by (A2). Asymptotically we find

$$
\begin{aligned}
\tau &= t - c + \mathcal{O}(t\, e^{-t}), \\
c &= \int_0^\infty d\tau\, \frac{[2P_1(0)\,\tau + P_1(0) + P_2(0)]\, e^{-\tau}}{1 - [2P_1(0)\,\tau + P_1(0) + P_2(0)]\, e^{-\tau}}.
\end{aligned}
$$

Substituting this into (A2) we arrive at

$$
\begin{aligned}
P_1(t) &= \Pi_1\, e^{-t} + \mathcal{O}(t\, e^{-2t}), \\
P_2(t) &= [2\Pi_1\, t + \Pi_2]\, e^{-t} + \mathcal{O}(t^2\, e^{-2t}),
\end{aligned}
$$

with $\Pi_1 = P_1(0)\, e^c$, and $\Pi_2 = [P_2(0) - 2cP_1(0)]\, e^c$.

In the complementary situation, $P_3(\tau^*) = 0$ at some τ^* and then it becomes negative. In the limit $\tau \to \tau^*$ the physical time diverges; see Eq. (A3). Therefore the range $\tau \geq \tau^*$ is physically forbidden so that the system reaches a fixed point (P_1^*, P_2^*), with

$$
\begin{aligned}
P_1^* &= P_1(0)\, e^{-\tau^*}, \\
P_2^* &= [2P_1(0)\,\tau^* + P_2(0)]\, e^{-\tau^*}.
\end{aligned}
$$

The approach to this fixed point is exponential in time.

The borderline between these two regimes occurs when $P_3(\tau) > 0$ for all $\tau \neq \tau^*$, i.e., the curve $P_3(\tau)$ touches the τ axis horizontally. Thus we require *both*

$$1 = [2P_1(0)\,\tau^* + P_1(0) + P_2(0)]\, e^{-\tau^*} \qquad (A4)$$

and

$$2P_1(0) = 2P_1(0)\,\tau^* + P_1(0) + P_2(0). \qquad (A5)$$

The second relation gives $\tau^* = [P_1(0) - P_2(0)]/[2P_1(0)]$. Substituting this into (A4) yields the separatrix

$$\frac{P_1(0) - P_2(0)}{2P_1(0)} = \ln 2P_1(0). \qquad (A6)$$

[1] W. Weidlich, *Sociodynamics: A Systematic Approach to Mathematical Modelling in the Social Sciences* (Harwood Academic Publihers, 2000).

[2] T. M. Liggett, *Interacting particle systems* (Springer-Verlag, New York, 1985).

[3] T. M. Liggett, *Stochastic interacting systems: contact, voter, and exclusion processes*, (Springer-Verlag, New York, 1999).

[4] P. L. Krapivsky, Phys. Rev. A **45**, 1067 (1992).

[5] S. Galam, Physica A **274**, 132 (1999).

[6] K. Sznajd-Weron and J. Sznajd, Int. J. Mod. Phys. C **11**, 1157 (2000).

[7] V. Spirin, P. L. Krapivsky, and S. Redner, Phys. Rev. E **63**, 036118 (2001).

[8] J. Holyst, K. Kacperski, and F. Schweitzer, in: *Annual Reviews of Computational Physics IX*, ed. D. Stauffer (World Scientific, Singapore 2001), pp. 253-273.

[9] D. Stauffer, J. Artif. Soc. Soc. Simul. **5**, no. 1 (2002).

[10] S. Galam, *cond-mat*/0211571.

[11] D. Neau, unpublished.

[12] G. Weisbuch, G. Deffuant, F. Amblard, and J. P. Nadal, *cond-mat*/0111494.

[13] A few other models with continuous opinion states were studied previously, see e.g., H. Föllmer, J. Math. Econ. **1**, 51 (1974); J. Kobayashi, J. Math. Sociology **24**, 285 (2001); R. Hegselmann and U. Krause, J. Artif. Soc. Soc. Simul. **5**, no. 3 (2002) and references therein.

[14] R. Axelrod, J. Conflict Resolution **41**, 203 (1997); R. Axelrod, *The complexity of cooperation* (Princeton University Press, 1997).

[15] C. Castellano, M. Marsili, and A. Vespignani, Phys. Rev. Lett. **85**, 3536 (2000); D. Vilone, A. Vespignani, and C. Castellano, Eur. Phys. J. B **30**, 399 (2002).

[16] E. Ben-Naim and P. L. Krapivsky, Phys. Rev. E **61**, R5 (2000).

[17] A. Baldassarri, U. M. B. Marconi, and A. Puglisi, Europhys. Lett. **58**, 14 (2001).

[18] P. A. Ferrari and L. R. G. Fontes, El. J. Prob. **3**, Paper no. 6 (1998).

[19] J. Krug and J. Garcia, J. Stat. Phys. **99**, 31 (2000).

[20] R. Rajesh and S. N. Majumdar, J. Stat. Phys. **99**, 943 (2000); Phys. Rev. E **64**, 036103 (2001).

[21] S. N. Coppersmith, C.-h. Liu, S. N. Majumdar, O. Narayan, and T. A. Witten, Phys. Rev. E **53**, 4673 (1996).

[22] Z. A. Melzak, *Mathematical Ideas, Modeling and Applications, Volume II of Companion to Concrete Mathematics* (Wiley, New York, 1976), p. 279.

[23] S. Ispolatov, P. L. Krapivsky, and S. Redner, Eur. Phys. J. B **2**, 267 (1998).

[24] J. M. Hammersley, in: *Proc. Sixth Berkley Symp. Math. Statist. Probab., Vol. 1* (University of California Press, 1972), pp. 345–394.

[25] D. Aldous and P. Diaconis, Probab. Theor. Rel. Fields **103**, 199 (1995).

[26] D. Zwillinger, *Handbook of Differential Equations* (Academic Press, London, 1989).

[27] M. J. Feigenbaum, J. Stat. Phys. **19**, 25 (1978).

[28] S. H. Strogatz, *Nonlinear Dynamics and Chaos* (Perseus, Cambridge, 1994).

[29] E. H. Lorentz, J. Atmos. Sci. **20**, 130 (1963).

[30] A. Novick-Cohen and L. A. Segal, Physica D, **10**, 277 (1984).

[31] L. Frachebourg, P. L. Krapivsky, and E. Ben-Naim, Phys. Rev. E **54**, 6186 (1996); L. Frachebourg and P. L. Krapivsky, J. Phys. A **31**, L287 (1998).

[32] F. Vazquez, P. L. Krapivsky, and S. Redner, J. Phys. A **36**, L61 (2003).